pH-Dependent cis → trans Isomerization Rates for Azobenzene Dyes in Aqueous Solution†

Nicholas J. Dunn, William H. Humphries IV,‡ Adam R. Offenbacher,‡ Travis L. King,§ and Jeffrey A. Gray*

Department of Chemistry and Biochemistry, Ohio Northern University, 525 S. Main Street, Ada, Ohio 45810

Received: April 3, 2009; Revised Manuscript Received: June 2, 2009

Azobenzenes can function as molecular switches driven by their unusual cis ↔ trans photoisomerization properties. The stability of an azobenzene-based switch depends on its rate of thermal relaxation, which is known to depend on the solvent environment, but few kinetic studies in aqueous media have been reported. We use nanosecond UV laser flash photolysis−transient absorption spectroscopy to measure thermal cis → trans isomerization rates for mono- and disubstituted *p*-aminoazobenzenes and *p*-hydroxyazobenzenes in water at 23 °C over the pH range of 4 to 11. Observed absorption transients are fit to first-order relaxation rate constants between 10^5 and 10^1 s^{-1}, which is generally much faster than in nonpolar solvents, and the relaxation rates vary systematically and predictably with pH as the equilibrium shifts to ionized forms of the dyes that isomerize much more rapidly. Acid ionization constants for these dyes determined from our kinetic mechanism are compared with the pH dependence of their equilibrium UV−vis spectra. New kinetics results may enable pH control of azobenzene-based molecular switching times.

Introduction

The molecular geometry of common azobenzene derivatives has been studied for more than 50 years, and acid−base ionization has been suggested to influence the interconvertability of trans and cis isomers of these dyes in solution.[1−6] The trans forms are expected to be more stable in the ground electronic state of all azobenzene dyes in solution, but electronic excitation using near-UV light can result in a significant degree of isomerization to the cis forms of the ground state. Rates for subsequent thermal cis → trans relaxation have been measured in various organic solvents using flash spectroscopic techniques,[7−11] and two distinct pathways, rotation and inversion, have been proposed to account for the large solvent and substituent dependences of the relaxation rate constants.[12−18] In particular, Whitten and coworkers reported several very detailed studies[8−10] showing that the most polarizable azobenzenes, such as 4-(diethylamino)-4′-nitroazobenzene (DENAB), which has both electron-donating and electron-accepting groups, are especially sensitive to solvent polarity and hydrogen bonding. They found that for dipolar dye molecules, the free energy of activation for cis → trans thermal isomerization, $\Delta G_{ct}^{\ddagger}$, correlates quantitatively with solvent Z values,[10] but they caution that these empirical correlations based on macroscopic solvent properties such as dielectric constants may fail to represent all specific molecular solvent−solute interactions. Sanchez and de Rossi[16] showed that azo isomerization rates depend on hydroxide ion concentration in water and mixed solvents. The effect of the local solvent environment on azo isomerization rates has remained in question, and very recent work has been directed toward polymeric environments.[18]

In this work, we report the first systematic study of absorption spectra and rates for thermal isomerization of azobenzene derivatives in aqueous solutions over a wide pH range. The rates we observe for several azobenzene dyes that undergo complete ionization in aqueous solutions are generally much faster than the isomerization rates for the same compounds in organic solvents. Following Sanchez and de Rossi,[16] we show that certain ionized (protonated or deprotonated) forms of the dyes have a much lower barrier to isomerization about the azo bond than neutral forms, and we propose a very general polyprotic acid−base equilibrium model to explain why our observed rate constants have strong, reversible, and sometimes cyclic variation with pH. In other words, thermal cis → trans isomerization of azo dyes can be either acid or base catalyzed, and this ionization reaction mechanism for the dyes in water enables quantitative prediction of isomerization rates.

It is well known that azo dyes do not readily dissolve in water. Several studies have shown that dimerization or more extensive aggregation can occur at relatively low concentrations (e.g., 10^{-4} mol/L) for some dye−solvent combinations.[19−24] In a very thorough spectrophotometric study, Reeves et al.[19] measured equilibrium constants for dimerization of sulfonated (ionic) azobenzenes in water with values on the order of 10^2 to 10^3 L/mol. More recent studies have shown that amphiphilic azo dyes linked to long-chain phospholipid[22] or sugar-terminated groups[24] can self-assemble into interesting H-aggregate structures. None of these aggregation studies included the simple amino- or hydroxy-substituted azobenzene compounds involved in our work. Krapfenbauer et al.[25] did, however, study oxidation kinetics following pulsed radiolysis for one of our compounds, 4-phenylazophenol, at similar concentrations in water and did not report evidence of dimer formation.

Photoisomerization of azobenzene-based structures has been the subject of many recent publications motivated by optomechanical molecular switching applications,[26−28] such as information storage in hydrophilic polymers[29−31] and transport through biomembranes.[32−35] Any specific design may require a molecular switch to be thermally stable on a time scale ranging

† Part of the "Robert W. Field Festschrift".

* Corresponding author. Tel: 419-772-2337. Fax: 419-772-2985. E-mail: j-gray@onu.edu.

‡ Current address: School of Chemistry and Biochemistry, Georgia Institute of Technology, Atlanta, GA 30332.

§ Current address: Department of Chemical and Biomolecular Engineering, University of Notre Dame, Notre Dame, IN 46556.

10.1021/jp903102u CCC: $40.75
Published on Web 07/20/2009

TABLE 1: Materials

substance name	abbrev.	CAS	init. pH
4-phenylazoaniline	M4AAB	60-09-3	2
4,4′-azodianiline	D4AAB	538-41-0	2
4-phenylazophenol	M4HAB	1689-82-3	12
4,4′-dihydroxy-azobenzene	D4HAB	2050-16-0	12
2,2′-dihydroxy-azobenzene	D2HAB	2050-14-8	12
4-(phenylazo)benzoic acid	M4CAB	1562-93-2	12
azobenzene-4,4′-dicarboxylic acid	D4CAB	586-91-4	12

from as short as nanoseconds to perhaps as long as many months. In some optical switching applications, trans → cis photoisomerization is reversed at some specific time later using light that has a different wavelength (usually longer),[28,34] and in these cases, reverse photoisomerization competes with thermal relaxation. Our new rate measurements and modeling may lead to a general understanding of how azobenzene dyes thermally isomerize in aqueous and other acid−base ionizing environments. The fact that these dye structures exhibit such dramatic, adjustable, and predictable relaxation behavior may enable new applications that use pH to control the response time of molecular switches actively.

Experimental Methods

In this study, we examined seven compounds having an azobenzene (AB) core structure. Table 1 lists a typical name and the CAS number for each substance. (The source and purity of each substance is listed in Table 1.S in the Supporting Information.) Each compound in this set is a mono- (M) or symmetrically di- (D)-substituted azobenzene involving either the amino (A), hydroxy (H), or carboxy (C) functional groups in the para (4) or ortho (2) positions. We use an abbreviation that indicates the number of, position of, and type of substituent; for example, M4AAB represents mono-4-aminoazobenzene. The compounds were all purchased and used without further purification.

Azobenzenes are generally rather insoluble in neutral water; however, each of the compounds in this study dissolves slowly at a pH that ionizes the functional group(s). pH adjustments were made using HCl(aq) or NaOH(aq), and the initial solution pH used to dissolve each compound is given in Table 1. Aqueous sample solutions having concentrations between 40 and 230 μM (±5%) were prepared using distilled−deionized water (15 MΩ) by warming to ca. 60 °C and stirring for 30 to 60 min. M4AAB, D4AAB, M4HAB, and D4HAB are metastable in solution for several weeks at any pH, whereas D2HAB, M4CAB, and D4CAB usually precipitate in only a few hours, especially when the pH is lowered.

An Ocean Optics model USB4000 spectrophotometer was used to record steady-state absorption spectra with 1.5 nm resolution in the range 200 to 800 nm for each substance in solution at various pH conditions. Spectra for several of these solutions were also recorded for comparison using a Shimadzu model 2400 scanning instrument to determine whether the absorptivity of these photosensitive dyes was altered by broadband excitation in the USB4000; however, no significant instrumental artifacts were observed.

For time-resolved experiments, test solutions were pumped through a 1 cm square quartz flow cell using a laser dye circulator having a capacity of 1 L. The flow rate through the cell was adjusted to between 1 and 4 mL/s using a bypass valve. The pH was adjusted during circulation until stable within ± 0.1 pH unit while being monitored continuously using a VWR model SP20 pH meter. All measurements were made at an ambient temperature of 23 ± 2 °C.

Our laser flash photolysis−transient absorption spectroscopy (LFP-TAS) and kinetics experiments employed a Quanta Ray model DCR-2A Q-switched Nd/YAG laser with a 355 nm output energy of 3 to 8 mJ/pulse operating at 1 to 10 Hz. The LFP beam was projected through a diffuser into a 4 × 10 mm region at the side of the sample flow cell. At this fluence, we estimate that up to 10% of the dye molecules undergo photoisomerization from the trans to the cis geometry during the 6 ns LFP pulses. The sample flow rate was sufficient to excite fresh sample on every pulse.

TAS experiments were performed using a small tungsten lamp whose output was collimated within a 4 mm diameter and directed perpendicular to the LFP beam crossing through the flow cell. The TAS beam then passed through a glass cutoff filter to reduce scattered LFP light and was imaged through a CVI model CM110 monochromator onto a photomultiplier tube. The monochromator bandpass was fixed at 16 nm for all experiments. TAS signals were conditioned using a preamp with bandwidth adjustable between 1 Hz and 1 MHz and were recorded using a Tektronix TDS3012B digital oscilloscope. We obtained transient spectra by adjusting the monochromator in 4 nm steps from 700 to 430 nm while recording a 128 shot average of the integrated signal gated over the initial 25% of the relaxation period. To determine isomerization rate constants, the monochromator was set at the wavelength for the maximum observed differential absorption, and 10k-point relaxation time traces were averaged for 512 shots. This LFP-TAS apparatus can monitor relaxation lifetimes from a few microseconds to more than 100 ms following photoisomerization. The slowest pulse repetition and sample flow rates were required to follow the longest relaxation times.

Results

Absorption spectra of azobenzenes at equilibrium generally have two or three strong, overlapping bands in the UV and visible regions. Figure 1 shows absorption spectra of aqueous solutions of M4AAB, D4AAB, M4HAB, and D4HAB at several pH values. All of these compounds are yellow in neutral solutions, but they show a noticeable color change to reddish orange when ionized (aminoazobenzenes at low pH and hydroxyazobenzenes at high pH) as the absorption feature at the longest wavelength is enhanced. All of the observed spectral changes with pH are reversible.

To address the question of dimer formation, we recorded absorption spectra of M4HAB and M4AAB at various concentrations, which shows that the absorptivity is slightly nonlinear. (See Figures 1.S−3.S in the Supporting Information.) These preliminary results, together with previously reported equilibrium constants for ionic azo dyes,[19] suggest that up to 10% of the dye molecules in our solutions may exist as dimers.

M4AAB has isosbestic points at 234, 272, 341, and 462 nm demarking spectra of distinct species that interconvert between pH 2 and 4. Recent calculations and resonance Raman spectra of M4AAB and its dimethylamino analog reported by Matazo et al.[36] show that the near-UV band, which appears here in Figure 1 with λ_{max} at 375 nm, should be assigned to neutral *trans*-M4AAB, whereas the bands we observe with λ_{max} at 500 and 316 nm should be assigned to the azo-protonated and amino-protonated tautomers of *trans*-M4AAB, respectively. Similarly, M4HAB has isosbestic points at 248, 290, and 370 nm demarking spectra of two distinct species that interconvert between pH 7 and 9. pH influences on the spectra of D4AAB

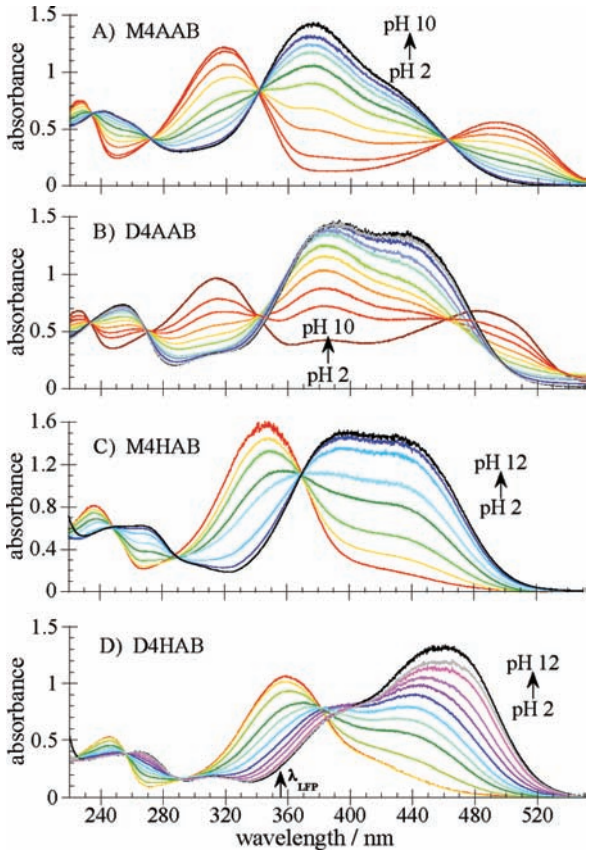

Figure 1. Equilibrium UV−vis absorption spectra of dilute azobenzene dye aqueous solutions show changes with pH typical of acid−base indicators. (A) 72 μM M4AAB at pH 1.63, 2.21, 2.53, 2.77, 3.01, 3.27, 3.52, 3.75, 4.53, and 10.50. (B) 72 μM D4AAB at pH 1.91, 2.22, 2.40, 2.62, 2.81, 3.03, 3.41, 3.60, 4.04, 4.54, and 10.50. (C) 80 μM M4HAB at pH 2.03, 7.16, 7.56, 8.00, 8.30, 8.75, 9.34, and 12.15. (D) 50 μM D4HAB at pH 2.01, 6.01, 7.27, 7.78, 8.03, 8.26, 8.52, 8.78, 9.04, 9.52, 10.07, and 12.30. The laser flash photolysis wavelength (λ_{LFP}) for transient experiments is indicated.

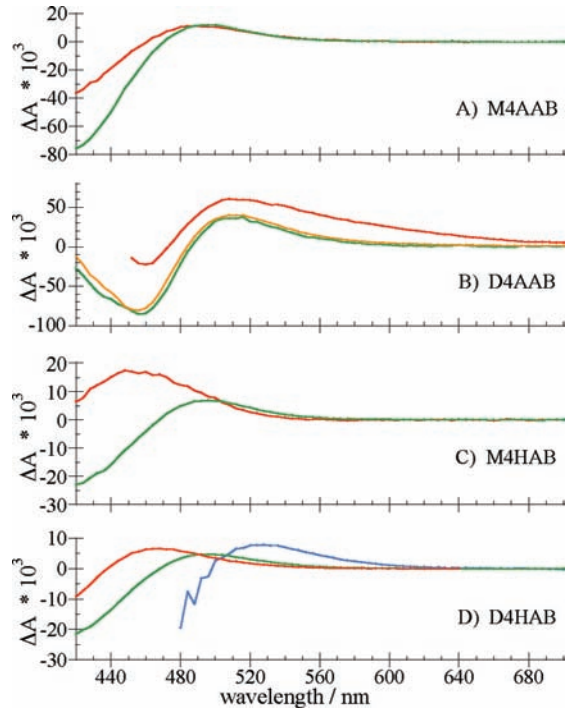

Figure 2. Transient UV−vis absorption spectra of dilute azobenzene dye aqueous solutions generally show an increase in long-wavelength absorbance following laser flash excitation at 355 nm. (A) 107 μM M4AAB at pH 4.9 and 6.6. (B) 106 μM D4AAB at pH 4.6, 5.8, and 6.6. (C) 204 μM M4HAB at pH 4.5 and 7.4. (D) 222 μM D4HAB at pH 5.4, 7.6, and 10.0. The spectrum of D4HAB at pH10.0 is truncated at 480 nm because of poor S/N.

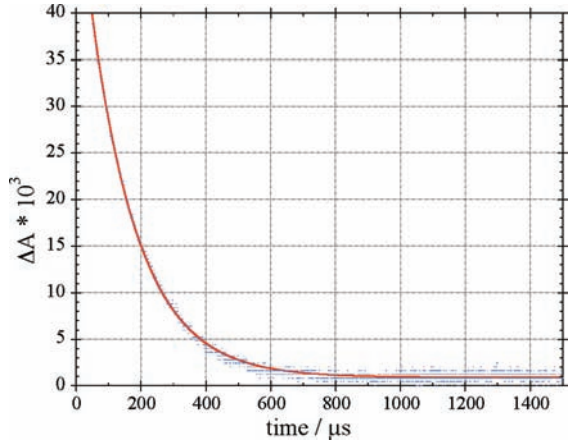

Figure 3. Observed transient absorbance at 500 nm for D4AAB at pH 4.57 follows first-order kinetics with a best fit 1/*e* lifetime of 149 μs.

and D4HAB generally resemble those of their monosubstituted counterparts, but for both disubstituted compounds, it appears that more than two species exist. In summary, all trans isomers of these azobenzene dyes appear to be yellow in color in neutral aqueous solution and change to reddish-orange, indicating acid or base ionization typical of the substituent group.

Although variation of functional groups, solvent, and pH generally causes equilibrium absorption bands to shift, trans isomers of all of the compounds in this study have molar absorptivity constants between 3000 and 21 000 L mol^{-1} cm^{-1} at 355 nm for all pH conditions. Flash irradiation at 355 nm thus increases the long-wavelength absorptivity due to the cis isomer for each substance. Figure 2 shows transient absorption spectra for aqueous solutions of M4AAB, D4AAB, M4HAB, and D4HAB at different pH values. Peak values of differential absorbance in the range of absorbance between 0.025 and 0.075 are consistent with a 10% maximum excitation efficiency estimated from LFP pulse fluence and an estimated branching ratio of 50% for the cis isomer upon return to the ground electronic state.[26] The absorbance change is largest at wavelengths near 500 nm for all of these compounds in neutral solution. Transient spectra of both aminoazobenzene compounds do not change much with pH, but λ_{max} for both hydroxyazobenzene compounds decreases to near 450 nm at lower pH. The transient spectra of all four compounds shift with pH in a qualitatively different way than their respective equilibrium spectra, which may imply that cis and trans isomers have different proton affinities.

Thermal cis → trans relaxation for all four compounds in our study obeys first-order kinetics under all pH conditions. Figure 3 shows an example transient absorption decay for D4AAB at pH 4.57. Data points for absorbance change, ΔA, beginning briefly after the LFP pulse fit very well to the time-decay expression $\Delta A_t = \Delta A_0 \times e^{-k_{obsd}t}$ + baseline with little systematic deviation. This is further evidence that most of the dissolved dye is in the form of individual molecules because significant dimerization would cause biexponential decays. Values of the observed relaxation rate constant k_{obsd} are precise and reproducible to within 5%. Relaxation rate constants strongly depend on pH and change reversibly as pH is raised

CHART 1: Quinoid-Like Resonance Structures

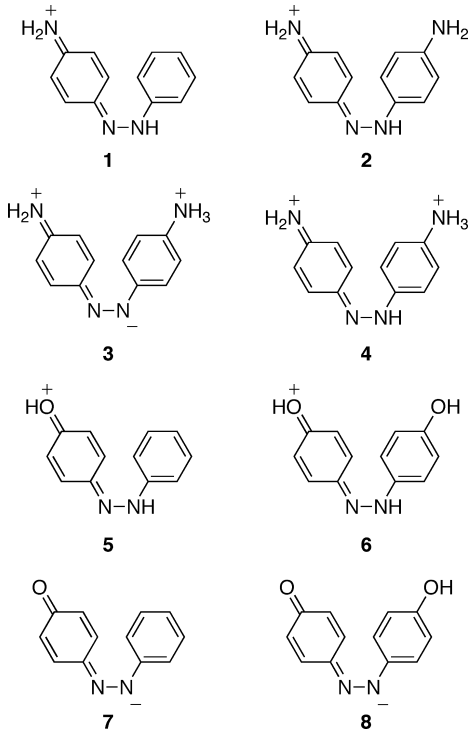

and lowered. However, we observe that these rate constants do not depend on LFP pulse energy or on the concentration of azobenzene dye in solution or on the amount of Na^+ and Cl^- added when adjusting the pH.

Table 2.S in the Supporting Information lists values of the measured relaxation rate constants for aqueous solutions of M4AAB, D4AAB, M4HAB, and D4HAB as a function of pH. The fastest observed rates for all compounds are at the lowest pH. The rate constants for both aminoazobenzene compounds reach a minimum asymptote value near 10^1 s^{-1} at higher pH, whereas the rate constants for both hydroxyazobenzene compounds show an unexpected cyclic variation with increasing pH.

Discussion

The structures of acid−base ionized forms of azobenzenes have been discussed in the literature since the earliest spectroscopic studies of these dyes in aqueous solutions.[1−6,16] To develop a general description of how pH affects azo dyes and to model our new rate measurements, we propose the following mechanism based on two primary assumptions: (1) the bond between the azo nitrogen atoms is easier to rotate about in certain ionized structures of each dye, and (2) the observed rate at any pH is the composite of two or more ionized forms in equilibrium undergoing thermal cis → trans isomerization through independent pathways having very different barriers. Unlike previous empirical correlations, this mechanism enables quantitative prediction of isomerization rates for dyes that ionize.

At low pH, all azobenzene compounds may be protonated at an azo position (azonium tautomer). M4AAB and D4AAB may also be protonated at an amino position (ammonium tautomers). Quantum chemical calculations[36,37] indicate that these tautomers have significantly different electronic structures and relative stabilities in solvents having different polarity, so solvation can affect their relative pK_a values. At high pH, hydroxyazobenzenes also undergo deprotonation at one or both of the hydroxyl groups. The relative energies and geometries for ionized forms of azobenzenes are likely to be different in water than in other solvents. Several ionic forms of these compounds have reasonably stable quinoid-like resonance structures, shown in Chart 1 below, that reduce the bond order for the azoic nitrogen atoms and thus have a smaller barrier to cis → trans thermal isomerization.

In aqueous solution, aminoazobenzenes and hydroxyazobenzenes should generally behave as polyprotic acids with cationic, neutral, and anionic forms in rapid, coupled equilibria. Although our observed isomerization rates for azo dyes are much faster than the corresponding rates in organic solvents, the very fast proton-transfer steps in water are expected to be at equilibrium on the time scale for azo isomerization. For each compound at a given pH, the relative concentration of ionized species is determined by a series of acid equilibrium constants. Our UV−vis absorption spectra of M4AAB and M4HAB each imply single ionization steps, and plots of our absorbance values versus pH have inflection points corresponding to pK_a values of 2.9 and 8.1, respectively. Klotz et al. reported[5] a similar pK_a value of 8.2 for M4HAB.

Faster isomerization rates are generally due to quinoid-like ionized forms rather than benzenoid[5] ionized forms of these dyes. Two relevant ionization constants therefore define the equilibria between doubly protonated (**4**) and singly protonated tautomers (**2** and **3**) and neutral forms of D4AAB

$$\mathrm{D4AABH_2^{2+}(aq) \rightleftarrows D4AABH^+(aq) + H^+(aq)} \quad K_{a1} \tag{1a}$$

and

$$\mathrm{D4AABH^+(aq) \rightleftarrows D4AAB(aq) + H^+(aq)} \quad K_{a2} \tag{1b}$$

For isomerization of M4AAB, the first and only significant ionization constant relates the protonated (**1**) and neutral forms

$$\mathrm{M4AABH^+(aq) \rightleftarrows M4AAB(aq) + H^+(aq)} \quad K_{a1} \tag{2a}$$

Isomerization of M4HAB involves ionic structures **5** and **7** and has a first ionization constant analogous to that defined in eq 2a as well as a second constant defined by

$$\mathrm{M4HAB(aq) \rightleftarrows M4HAB^-(aq) + H^+(aq)} \quad K_{a2} \tag{2b}$$

Finally, fast isomerization of D4HAB at low and slightly basic pH involves the quinoid ionic structures **6** and **8**. Isomerization of D4HAB becomes slow at high pH, suggesting that $D4HAB^{2-}$ has a less favorable isomerization pathway because **9** is a much less significant structure than **10**.

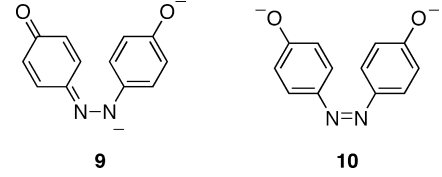

D4HAB therefore has first and second constants analogous to those defined by eqs 2a and 2b as well as a third constant defined by

$$\mathrm{D4HAB^-(aq) \rightleftarrows D4HAB^{2-}(aq) + H^+(aq)} \quad K_{a3} \tag{2c}$$

For D4AAB at a given pH, the fractions of total concentration, α, expected for each stage of ionization defined by eq 1a and 1b above may be computed by applying the following standard set of equations that generally describe coupled acid−base equilibria[16,38,39]

$$\alpha_{2+} \equiv \frac{[\mathrm{D4AABH^{2+}}]}{[\mathrm{D4AAB}]_{tot}} = \left[1 + \frac{K_{a1}}{[H^+]} + \frac{K_{a1}K_{a2}}{[H^+]^2}\right]^{-1} \tag{3a}$$

$$\alpha_{+} \equiv \frac{[\mathrm{D4AABH^{+}}]}{[\mathrm{D4AAB}]_{tot}} = \left[1 + \frac{[H^+]}{K_{a1}} + \frac{K_{a2}}{[H^+]}\right]^{-1} \tag{3b}$$

and

$$\alpha_{0} \equiv \frac{[\mathrm{D4AAB}]}{[\mathrm{D4AAB}]_{tot}} = \left[1 + \frac{[H^+]^2}{K_{a1}K_{a2}} + \frac{[H^+]}{K_{a2}}\right]^{-1} \tag{3c}$$

For our other three compounds, whose distribution of ionized species begins instead with the monocation, the fractions of total concentration at a given pH, α, existing for each stage of ionization defined by eqs 2a−2c above may be computed using the equivalent series of equations

$$\alpha_{+} \equiv \frac{[\mathrm{ABH^{+}}]}{[\mathrm{AB}]_{tot}} = \left[1 + \frac{K_{a1}}{[H^+]} + \frac{K_{a1}K_{a2}}{[H^+]^2} + \frac{K_{a1}K_{a2}K_{a3}}{[H^+]^3}\right]^{-1} \tag{4a}$$

$$\alpha_{0} \equiv \frac{[\mathrm{AB}]}{[\mathrm{AB}]_{tot}} = \left[1 + \frac{[H^+]}{K_{a1}} + \frac{K_{a2}}{[H^+]} + \frac{K_{a2}K_{a3}}{[H^+]^2}\right]^{-1} \tag{4b}$$

$$\alpha_{-} \equiv \frac{[\mathrm{AB^-}]}{[\mathrm{AB}]_{tot}} = \left[1 + \frac{[H^+]^2}{K_{a1}K_{a2}} + \frac{[H^+]}{K_{a2}} + \frac{K_{a3}}{[H^+]}\right]^{-1} \tag{4c}$$

and

$$\alpha_{2-} \equiv \frac{[\mathrm{AB^{2-}}]}{[\mathrm{AB}]_{tot}} = \left[1 + \frac{[H^+]^3}{K_{a1}K_{a2}K_{a3}} + \frac{[H^+]^2}{K_{a2}K_{a3}} + \frac{[H^+]}{K_{a3}}\right]^{-1} \tag{4d}$$

Because only D4HAB requires all three of these ionization constants, eqs 4a−4d are modified to apply to M4AAB and M4HAB by removing terms involving unnecessary K_a values; for example, M4AAB requires only eqs 4a and 4b without the terms having K_{a2} and K_{a3}. For any compound at a given pH, the sum of all composition fractions α is unity. It is important to realize that the form of eqs 3a−3c and 4a−4d applies to any polyprotic acid system and is not unique to the azo dyes in our study.

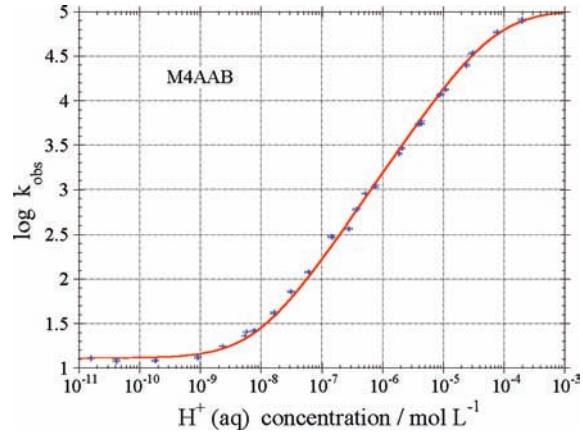

Figure 4. Observed decay rate coefficients for M4AAB fit well to an isomerization kinetic model assuming rapid acid−base equilibrium between neutral and protonated (azonium) forms of the dye in solution. Isomerization rates at neutral and higher pH decrease in proportion to the predicted azonium concentration.

The general kinetic mechanism for thermal cis → trans isomerization of an azobenzene dye involves multiple pathways with a distinct rate coefficient for each stage of ionization. Here we consider two (M4AAB), three (D4AAB and M4HAB), or four (D4HAB) pathways.

$$\begin{array}{lccccccccc} \text{cis:} & \mathrm{ABH_2^{2+}} & \rightleftarrows & \mathrm{ABH^+} & \rightleftarrows & \mathrm{AB} & \rightleftarrows & \mathrm{AB^-} & \rightleftarrows & \mathrm{AB^{2-}} \\ \downarrow k_{obsd}\text{:} & \downarrow k_{2+} & & \downarrow k_{+} & & \downarrow k_{0} & & \downarrow k_{-} & & \downarrow k_{2-} \\ \text{trans:} & \mathrm{ABH_2^{2+}} & \rightleftarrows & \mathrm{ABH^+} & \rightleftarrows & \mathrm{AB} & \rightleftarrows & \mathrm{AB^-} & \rightleftarrows & \mathrm{AB^{2-}} \end{array} \tag{5}$$

For each dye, we model the observed relaxation rate constant k_{obsd} at a given pH as the sum of rate coefficients for its ionized species times the fraction of each species present at that pH

$$k_{obsd} = \alpha_{2+}k_{2+} + \alpha_{+}k_{+} + \alpha_{0}k_{0} + \alpha_{-}k_{-} + \alpha_{2-}k_{2-} \tag{6}$$

Figure 4 shows data for M4AAB from Table 2.S in the Supporting Information plotted with least-squares fits to the model described above. M4AAB is the simplest case because it involves only one ionization constant and two rate coefficients k_+ and k_0. The best fit value for K_{a1} in Table 2 corresponds to $pK_{a1} = 4.17$, which is somewhat different than the value (2.9) determined from our optical absorbance measurements, possibly because the ammonium and azonium tautomers may coexist, because cis and trans geometries have different pK_a values, or both. In Figure 4, it may seem surprising that k_{obsd} reaches the asymptotic value of k_0 above pH ~8 given that pK_{a1} is near 4, but k_{obsd} is dominated by k_+ for even small relative concentrations α_+ because the value of k_+ is approximately 10^4 times larger than that of k_0. The relative size of these rate coefficients at 296 K implies that acid catalysis effectively lowers the cis → trans thermal isomerization barrier, that is, the activation free energy, $\Delta G_{ct}^{\ddagger}$, by as much as 20 to 25 kJ/mol, which is consistent with the azonium form including a significant resonance contribution from structure **1** and therefore having a somewhat lower N−N bond order. The linear relationship between $\Delta G_{ct}^{\ddagger}$ and pH for M4AAB as well as our other dyes,

TABLE 2: Fitted Ionization Constants and Rate Coefficients for the Acid−Base Model

parameter	M4AAB	D4AAB	M4HAB	D4HAB
K_{a1}	$(6.8 \pm 0.6)^a \times 10^{-5}$	$(3.02 \pm 0.04) \times 10^{-4}$	$(3.76 \pm 0.06) \times 10^{-4}$	$(2.03 \pm 0.04) \times 10^{-4}$
K_{a2}		$(4.6 \pm 0.6) \times 10^{-5}$	$(7 \pm 4) \times 10^{-9}$	$(3.9 \pm 0.2) \times 10^{-9}$
K_{a3}				$(9.1 \pm 0.6) \times 10^{-10}$
k_{2+}/s^{-1}		$(5.9 \pm 0.6) \times 10^{+4}$		
k_+/s^{-1}	$(1.06 \pm 0.08) \times 10^{+5}$	$\{5 \times 10^{+4}\}^b$	$\{2 \times 10^{+5}\}$	$\{2 \times 10^{+5}\}$
k_0/s^{-1}	12.9 ± 0.4	{20}	108 ± 21	110 ± 16
k_-/s^{-1}			$(6 \pm 5) \times 10^{+3}$	$(9.4 \pm 0.3) \times 10^{+3}$
k_{2-}/s^{-1}				11 ± 2
K_{inh}			$(9 \pm 9) \times 10^{-5}$	$\{5 \times 10^{-9}\}$
$[H^+]_{inh}$			$(4 \pm 1) \times 10^{-6}$	$\{1.3 \times 10^{-9}\}$

[a] Uncertainty estimates are one standard deviation. [b] Constants in brackets {} were held fixed in the final fit.

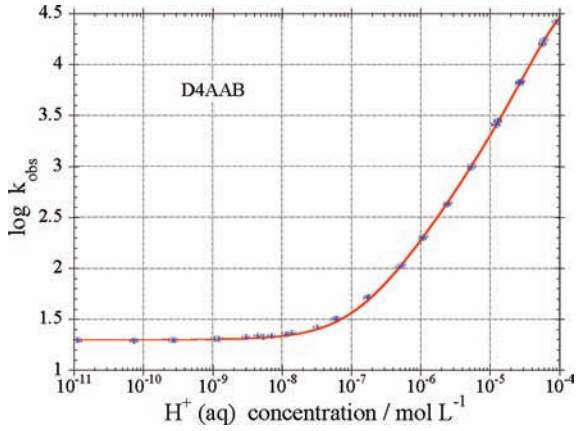

Figure 5. Observed decay rate coefficients for D4AAB fit well to an isomerization kinetic model assuming rapid acid−base equilibrium between neutral, protonated (azonium), and diprotonated (azonium, ammonium) forms of the dye in solution. Isomerization rates at neutral and higher pH decrease with predicted ionic concentrations.

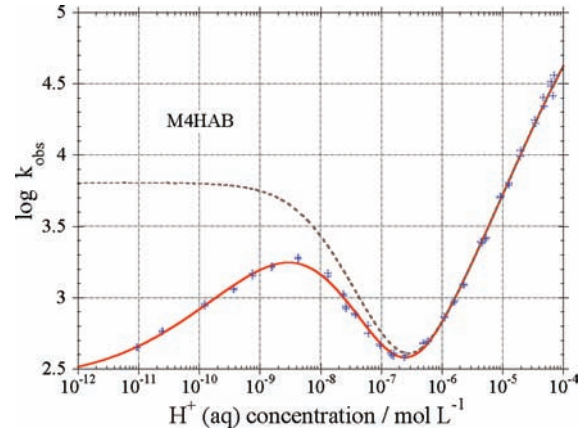

Figure 6. Observed decay rate coefficients for M4HAB at pH below ~ 8 fit well to an isomerization kinetic model assuming rapid acid−base equilibrium between protonated (azonium), neutral, and deprotonated anionic forms of the dye in solution. The observed decrease in isomerization rate above pH 9 is not accounted for by the acid−base model alone (dashed line), but rather these values fit an empirical power-law expression with a weaker dependence on $[H^+]$.

which is displayed by slopes near unity over wide pH ranges in Figures 4−7, illustrates that an acid−base catalysis mechanism quantitatively applies to these dyes in water.

Figure 5 shows data and model results for D4AAB with fitted constants listed in Table 2. The best fit value of pK_{a2} for D4AAB, 4.34, is similar to that for the equivalent stage of ionization of M4AAB ($pK_{a1} = 4.17$), as described above. k_{obsd} values for D4AAB approach an upper limit like those for M4AAB, but this limit is less noticeable at pH 4 for D4AAB because k_{2+} and k_+ both contribute to the maximum value for k_{obsd} and because $pK_{a1} = 3.52$ is below this range. This aspect of our data for D4AAB also causes k_{2+} and k_+ to be correlated, so we held the parameters k_+ and k_0 fixed in the final fit, yet the k_{2+} value has a large relative uncertainty.

Figure 6 shows data and model results for M4HAB with values for fitted constants listed in Table 2. For M4AHB, our acid−base catalysis mechanism properly describes how k_{obsd} decreases from pH 4 to 6.5 then increases from pH 6.5 to 8.3. At higher pH, our equilibrium model predicts that k_{obsd} should become constant and equal to k_-, as indicated by the dashed line in Figure 6. However, our data clearly show k_{obsd} values decreasing, though more gradually, above pH 8.3 where the anion is the predominant form. Fitting the data in this range requires that k_- decreases with increasing pH, and the functional form follows the equation

$$k_{-\,\mathrm{eff}} = \frac{k_-}{1 + (K_{inh}/(\sqrt{[H^+]} + [H^+]_{inh}))} \qquad (7)$$

with two additional empirical parameters K_{inh} and $[H^+]_{inh}$ that represent this inhibition of k_-. The possible physical significance of these parameters is unknown, and they are correlated with k_- and K_{a2}, which causes all of these fitted values to have relatively larger uncertainties.

The azonium form of M4HAB has the largest rate coefficient because of its lower isomerization barrier, and the values of k_+ and k_0 for M4HAB are similar to those for M4AAB and D4AAB. The best-fit value for the first ionization constant of M4HAB, $pK_{a1} = 3.42$, supports the expectation that an azophenol should not be as basic as an azoaniline. The best-fit value for deprotonation, $pK_{a2} = 8.2$, is lower than that for most phenols. The resulting value for k_- is somewhat larger than k_0, which implies that isomerization is base-catalyzed, although not as effectively as by acid.

In 1968 Gabor et al.[40] reported that the isomerization rate of M4HAB depends strongly on temperature, concentration, and solvent. They postulated that in nonpolar solvents (methylcyclohexane and benzene), dimers readily form at concentrations of 30 μM and cause the relaxation kinetics to deviate from first order, but in polar solvents (alcohol), the solvent−solute interactions are strong enough to prevent aggregation. In 2005, Kojima et al.[41] studied hydrogen bonding and acid effects on the isomerization rates of M4HAB in organic solvents and performed ab inito calculations of solvation structures to support the postulated role of dimerization on the rates. They concluded that solvation in methanol and acetonitrile is strong enough to suppresses dimer formation and that H-bonding between these solvents and M4HAB causes its isomerization rate to increase.

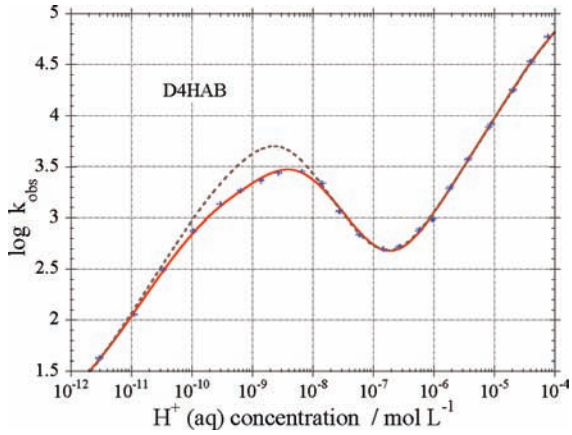

Figure 7. Observed decay rate coefficients for D4HAB at pH below ~ 8 and above ~ 10 fit well to an isomerization kinetic model assuming rapid acid−base equilibrium between protonated (azonium), neutral, anionic, and dianionic forms of the dye in solution. The disagreement between observed rates and the acid−base model (dashed line) for pH between 8 and 10 where the anionic form that has the greatest concentration is similar to that observed for M4AHB and can be fit well (solid line) by adding an empirical term to the model that effectively sequesters the monoanion concentration.

Therefore, it appears that our observed decrease in isomerization rate for M4HAB above pH 8 is more likely caused by reduced solvent interaction than by dimerization.

Figure 7 shows data and model results for D4HAB with fitted constants in Table 2. The best-fit values for k_+, k_0, k_-, K_{a1}, and K_{a2} may be interpreted in much the same way as the corresponding constants for M4HAB. An empirical inhibition of the k_- term is again required, although the effect is only apparent over the limited pH range, where α_- has a significant value. As with M4HAB, this inhibition in D4HAB is more likely caused by changing solvent interactions than by aggregation. The best-fit values for K_{a2} and K_{a3}, which represent successive deprotonation steps, are surprisingly not very different, which may imply that there is little or no conjugation coupling of the two rings. Our preliminary computational results indicate a significantly nonplanar structure for *cis*-D4HAB, which supports this lack of conjugation. The best-fit value for k_{2-} is much more similar to values of rate coefficients for neutral species than to those for other ionic species. This observation may be understood as a relatively minor contribution by the quinoid structure **9** such that the dianion **10** has complete azo π-bond character like the neutral species.

Some azo dyes other than those studied here would also be expected to exhibit the general effects of acid−base catalysis in solution. Because *para*-alkylamino derivatives of azobenzene have such similar electronic structure, spectra, and acid−base properties,[3,36,37,42] they could have pH-dependent isomerization rates very similar to those we observe for M4AAB and D4AAB. Likewise, isomerization of aqueous *para*-alkoxyazobenzenes may follow the trends seen here for M4HAB and D4HAB at low and neutral pH but not at higher pH because alkoxy quinoid-like structures cannot be stabilized by deprotonation. Asymmetric derivatives such as 4-amino-4′-hydroxy azobenzene may also have isomerization rates similar to those we report here. Conversely, common derivatives having only nitro, nitrile, acid, and ester groups would not be expected to have enhanced isomerization in any pH range.

Some applications such as data storage in polymer films[29,31] that employ photomechanical isomerization of azobenzenes require very slow thermal cis → trans relaxation rates (i.e., lifetimes of hours to months). Other applications such as biofunctional materials[32] require more rapid relaxation rates, and in these systems, it may be possible to achieve control of the cis lifetime simply by adjusting the pH rather than by actively resetting the molecular switch with another pulse of light.

Conclusions

Novel laser flash photolysis−transient absorption spectroscopy experiments have shown that the rate of thermal cis → trans isomerization for aminoazobenzene and hydroxyazobenzene dyes in aqueous solution is strongly dependent on pH. Some ionized forms of these dyes in water have rate constants that are 10^4 times larger than the neutral forms, and the apparent isomerization rate at a given pH can be quantitatively predicted using a mechanism with the relative concentrations of ionic and neutral forms determined by acid−base equilibrium. Some acid equilibrium constants (K_a) determined from variations of UV−vis absorptivity of the trans isomer differ from those governing isomerization kinetics because enhancement of rates is due only to ionic tautomers involving the azo bond and because the cis isomers are likely to have different K_a values.

Acknowledgment. This work was made possible by generous support from Research Corporation award CC5910/5721 and a large laser donated by Professor Robert W. Field (MIT). Drs. Tevye C. Celius and Jake R. Zimmerman (ONU) contributed through many very helpful discussions, and Joshua E. Szekely recorded absorption spectra for the Supporting Information.

Supporting Information Available: Table of materials with sources and purity, numeric values for observed cis → trans thermal relaxation rate coefficients, absorption spectra of M4HAB and M4AAB as a function of concentration, and plots of absorbance versus concentration for M4HAB and M4AAB at varying pH. This material is available free of charge via the Internet at http://pubs.acs.org.

References and Notes

(1) Brode, W. R.; Gould, J. H.; Wyman, G. M. *J. Am. Chem. Soc.* **1952**, *74*, 4641.
(2) Birnbaum, P. P.; Style, W. G. *Trans. Faraday Soc.* **1954**, *50*, 1192.
(3) Sawicki, E. *J. Org. Chem.* **1957**, *22*, 365.
(4) Yeh, S.-J.; Jaffe, H. H. *J. Am. Chem. Soc.* **1959**, *81*, 3279.
(5) Klotz, I. M.; Fiess, H. A.; Chen Ho, J. Y.; Mellody, M. *J. Am. Chem. Soc.* **1954**, *76*, 5136.
(6) Gabor, G.; Fischer, E. *J. Phys. Chem.* **1962**, *66*, 2478.
(7) Gegiou, D.; Muszkat, K. A.; Fischer, E. *J. Am. Chem. Soc.* **1968**, *90*, 3907.
(8) Wildes, P. D.; Pacifici, J. G.; Irick, G., Jr.; Whitten, D. G. *J. Am. Chem. Soc.* **1971**, *93*, 2004.
(9) Schanze, K. S.; Mattox, T. F.; Whitten, D. G. *J. Am. Chem. Soc.* **1982**, *104*, 1733.
(10) (a) Schanze, K. S.; Mattox, T. F.; Whitten, D. G. *J. Org. Chem.* **1983**, *48*, 2808. (b) Kosower, E. M. *J. Am. Chem. Soc.* **1958**, *80*, 3253. (c) Kosower, E. M. *J. Am. Chem. Soc.* **1958**, *80*, 3267.
(11) Mukherjee, S.; Bera, S. C. *J. Chem. Soc., Faraday Trans.* **1998**, *94*, 67.
(12) Asano, T.; Okada, T. *J. Org. Chem.* **1984**, *49*, 4387.
(13) Asano, T.; Okada, T. *J. Org. Chem.* **1986**, *51*, 4454.
(14) Shaababi, A.; Zahedi, M. *J. Mol. Struct.* **2000**, 257.
(15) Fujino, T.; Arzhantsev, S. Y.; Tahara, T. *J. Phys. Chem. A* **2001**, *105*, 8123.
(16) Sanchez, A. M.; de Rossi, R. H. *J. Org. Chem.* **1995**, *60*, 2974.
(17) Fu, J.; Lau, K.; Barra, M. *J. Org. Chem.* **2009**, *74*, 1770.
(18) (a) Ho, C.-H.; Yang, K.-N.; Lee, S.-N. *J. Polym. Sci., Part A: Polym. Chem.* **2001**, *39*, 2296. (b) Serra, F.; Terentjev, E. M. *Macromolecules* **2008**, *41*, 981.
(19) Reeves, R. L.; Maggio, M. S.; Harkaway, S. A. *J. Phys. Chem.* **1979**, *83*, 2359.
(20) Heesemann, J. *J. Am. Chem. Soc.* **1980**, *102*, 2167.
(21) Hamada, K.; Iijima, T.; Amiya, S. *J. Phys. Chem.* **1990**, *94*, 3766.
(22) Song, X.; Perlstein, J.; Whitten, D. G. *J. Am. Chem. Soc.* **1997**, *119*, 9144.

(23) Xie, H.; Liu, L.; Wang, W.; Xu, L. *Chem. Phys. Lett.* **2005**, *403*, 175.
(24) Narayan, G.; Kumar, N. S. S.; Paul, S.; Srinivas, O.; Jayaraman, N.; Das, S. *J. Photochem. Photobiol., A* **2007**, *189*, 405.
(25) Krapfenbauer, K.; Wolfger, H.; Getoff, N.; Hamblett, I.; Navaratnam, S. *Radiat. Phys. Chem.* **2000**, *58*, 21.
(26) Blevins, A.; Blanchard, G. J. *J. Phys. Chem. B* **2004**, *108*, 4962.
(27) Comstock, M. J.; Levy, N.; Kirakosian, A.; Cho, J.; Lauterwasser, F.; Harvey, J. H.; Strubbe, D. A; Frechet, J. M. J.; Trauner, D; Louie, S. G.; Crommie, M. F. *Phys. Rev. Lett.* **2007**, *99*, 038301.
(28) Yager, K. G.; Barrett, C. J. *J. Photochem. Photobiol., A* **2006**, *182*, 250.
(29) Imaizumi, D.; Hayakawa, T; Kasuga, T.; Nogami, M. *J. Sol−Gel Sci. Technol.* **2000**, *19*, 383.
(30) Antonov, L.; Kamada, K.; Ohta, K.; Kamounah, F. S. *Phys. Chem. Chem. Phys.* **2003**, *5*, 1193.
(31) Petrova, S. S.; Chichinadze, N. M.; Shaverdova, V. G. *Tech. Phys.* **2005**, *50*, 227.
(32) Willner, I. *Acc. Chem. Res.* **1997**, *30*, 347.
(33) Sata, T.; Shimokawa, Y.; Matsusaki, K. *J. Membr. Sci.* **2000**, *171*, 31.
(34) Volgraf, M.; Gorostiza, P.; Szobota, S.; Helix, M. R.; Isacoff, E. Y.; Trauner, D. *J. Am. Chem. Soc.* **2007**, *129*, 260.
(35) Qu, W.; Tan, H.; Chen, G.; Liu, R. *Phys. Chem. Chem. Phys.* **2003**, *5*, 2327.
(36) Matazo, D. R. C.; Ando, R. A.; Borin, A. C.; Santos, P. S. *J. Chem. Phys. A* **2008**, *112*, 4437.
(37) Liwo, A.; Tempczyk, A.; Widernik, T.; Klentak, T.; Czerminski, J. *J. Chem. Soc., Perkin Trans. 2* **1994**, 71.
(38) Pietrzyk, D. J.; Frank, C. W. *Analytical Chemistry*, 2nd ed.; Academic Press: New York, 1979; p 374.
(39) Skoog, D. A.; West, D. M.; Holler, F. J.; Crouch, S. R. *Fundamentals of Analytical Chemistry*, 8th ed.; Thomson Brooks/Cole: Belmont, CA, **2004**; p 420.
(40) Gabor, G.; Frei, Y. F.; Fisher, E. *J. Phys. Chem.* **1968**, *72*, 3266.
(41) Kojima, M.; Nebashi, S.; Ogawa, K.; Kurita, N. *J. Phys. Org. Chem.* **2005**, *18*, 994.
(42) Barker, I. K.; Faucett, V.; Long, D. A. *J. Raman Spectrosc.* **1987**, *18*, 71.

JP903102U